Electronic Supplementary Material (ESI) for Nanoscale.
This journal is © The Royal Society of Chemistry 2019

# Supplementary Material (ESI) for

# Tailoring adhesion of anionic surfaces using cationic PISA-latexes – towards tough nanocellulose materials in the wet state

J. Engström[a,b] T. Benselfelt[a,b], L. Wågberg[a,b], F. D'Agosto[c], M. Lansalot[c], A. Carlmark[a,d]* and E. Malmström[a]*

[a] *KTH Royal Institute of Technology, School of Chemistry, Biotechnology and Health, [a]Department of Fibre and Polymer Technology, [b]Wallenberg Wood Science Center, SE-100 44, Stockholm, Sweden*

[c] *Université de Lyon, Univ Lyon 1, CPE Lyon, CNRS UMR 5265, C2P2 (Chemistry, Catalysis, Polymers & Processes), LCPP, 69616 Villeurbanne, France*

[d]*Presently at RISE Research Institutes of Sweden AB, Drottning Kristinas Väg 61, 114 28, Stockholm Sweden*

** Corresponding author e-mail: anna.carlmark@ri.se and mavem@kth.se*

## Contents

1. Instrumentation and methods ..... 1
2. Analysis of macroRAFT agent PDMAPMA ..... 3
3. Analysis of PMMA, P(BA-co-MMA) and PBA latexes during synthesis and dispersions ..... 5
4. Work-up protocol for removal of free PDMAPMA-chains ..... 8
5. Adsorption in QCM-D of latexes on silica surfaces..... 10
6. Adsorption of latexes on a CNF layer formed *in situ* with the aid of QCM-D ..... 12
7. Adsorption of latexes on a CNF layer formed *ex situ* on silica wafers ..... 13
8. Adsorption of latexes to clean glass substrates ..... 14
9. Adsorption of latexes on filter paper ..... 15

## 1. Instrumentation and methods

**Nuclear magnetic resonance (NMR):** The polymerization of DMAPMA was monitored by $^1$H-NMR with a Bruker Avance AM 400 NMR instrument using $D_2O$ as solvent. For the estimation of conversion of the monomer and for the degree of hydrolysis, 1,3,5-trioxane was used as an internal reference. The final latex particles were analyzed with $^1$H-NMR to analyze the final structure after freeze-drying and dissolution in $CDCl_3$. In order to establish a calibration curve for macroRAFT PDMAPMA, samples of known concetrations 0.3, 6 and 19 g $L^{-1}$ were run in $D_2O$ and intensity values for peaks at 2.8 and 3.1 ppm were used as data points, see ESI Figure S3.

**Maldi-ToF MS:** Matrix assisted laser desorption ionization-time of flight mass spectrometry (MALDI-ToF MS). Mass spectra were acquired on a Voyager-DE STR (Applied Biosystems, Framingham, MA). This instrument was equipped with a nitrogen laser (wavelength 337 nm) to desorb and ionize the samples. Samples were analysed using 2,5-dihydroxybenzoic acid (DHB) as matrix. The accelerating voltage used was 20 kV. The spectra were the sum of 300 shots, and an external mass calibration was used. Samples were prepared by dissolving the polymer in $H_2O$ at a concentration of 10 g $L^{-1}$.

**Gravimetric analysis:** The conversion of monomers during the emulsion polymerization was monitored gravimetrically; samples were withdrawn at different reaction times and dried in fume hood overnight, allowing the dry content to be calculated from residual solid material.

**Size exclusion chromatography (SEC):** The analysis of the number-average molar mass ($M_n$), weight-average molar mass ($M_w$) and dispersity ($Đ_M$) for polymers and latexes were determined by SEC using either water and buffer (0.3 M sodium acetate/acetic acid buffer), THF, DMF or DMSO as the mobile phase. The water SEC with buffer (0.3 M buffer sodium acetate/acetic acid buffer) was ran with a HPLC-pump Waters 510 (Millipore) equipped with a RID-10 RI-detector (Shimadzu) and ran at 35 °C with a flow rate of 0.5 mL $min^{-1}$ using three TSK gel columns G 3000 PWxl , 6000 PWxl together with a guard column (TOSOH), conventional calibration with PEG and PEO standards. The THF SEC was ran with a GPCMAX and autosampler from Malvern Instruments equipped with RI detector and ran at 35 °C with a flow rate of 1 mL $min^{-1}$ using guard column TGuard and two linear mixed bead columns LT4000L, conventional calibration with polystyrene standards. The DMF SEC was ran with a TOSOH EcoSEC HLC-8320GPC system equipped with an EcoSEC RI detector and three columns (PSS PFG 5 µm; Microguard, 100 Å, and 300 Å; MW resolving range: 100-300 000 g $mol^{-1}$) from PSS GmbH, using DMF with 0.01 M LiBr as the mobile phase at 50 °C with a flow rate of 0.2 mL $min^{-1}$. A conventional calibration method with PMMA standards ranging from 700 to 2 000 000 g $mol^{-1}$ was used. The DMSO SEC was ran with a SECcurity 1260 (PSS, Mainz, Germany) equipped with RI detector (40 °C), UV-VIS detector and three columns (PSS GRAM; precolumn, 10 µm 100 Å and 10 µm 10000 Å), using DMSO + 0.5 w/w% LiBr as the mobile phase at 60 °C and a flow rate of 0.5 mL $min^{-1}$. A conventional calibration method was used, employing pullulan standards. All samples were freeze-dried prior to dilution in the mobile phase before injection. Corrections for flow rate fluctuations were made using internal standards.

**Differential scanning calorimetry (DSC):** DSC analysis was performed with a Mettler Toledo DSC. All latex particles and the macroRAFT were analyzed with heating and cooling rate of 10 °C $min^{-1}$ in nitrogen atmosphere. The latexes were freeze-dried prior to analysis, and macroRAFT used as is after purification and drying. The method used was heating from -60 to 150 °C, equilibrium for 5 min and

then cooling from 150 to -60 °C, equilibrium for 5 min and a second heating from -60 to 150 °C. Data from the second heating were used to calculate the glass transition temperature ($T_g$) for all samples.

**Polyelectrolyte titration (PET):** The inherent charge density was measured in MilliQ water for all latex particles and the hydrophilic macroRAFT with a PET using a 716 DMS Titrino (Metrohm, Switzerland) with potassium poly(vinyl sulfate) (KPVS) as the titrant and ortho-toluidine blue (OTB) as the indicator. The change in color was recorded with a Fotoelektrischer Messkopf 2000 (BASF) and the amount of KPVS needed to titrate to equilibrium was calculated according to a method described by Horn *et al.*[62]

**Fourier transform infrared spectroscopy (FTIR):** Infrared spectra of filter papers with adsorbed latexes from water or 10 mM NaCl dispersions were recorded with a Perkin-Elmer Spectrum 2000 FT-IR equipped with a MKII Golden Gate, single reflection ATR System (from Specac Ltd., London, U.K.). The utilized ATR-crystal was a MKII heated Diamond 45° ATR Top Plate. All samples were analyzed by 16 scans, two or more times to achieve a representative curve and normalized to the crystal region at 2350 to 1900 $cm^{-1}$.

## 2. Analysis of macroRAFT agent PDMAPMA

The conversion of DMAPMA during RAFT synthesis in water at neutral pH was followed by the disappearance of vinyl peaks at 5.3 and 5.6 ppm using 1,3,5-trioxane as internal reference. $^1$H-NMR spectrum of the final polymer is shown in Figure S1, and monomer conversion versus time in Figure S2. The signal of the hydrogens on the RAFT-agent propyl end group is difficult to fully distinguish, due to the region of methyl in PDMAPMA polymer repeating unit and backbone around 0.75 to 1.1 ppm. But one can calculate a degree of polymerization from protons next to carboxyl group in the RAFT group at 2.2-2.3 ppm (b) or 2.65-2.7 ppm (a), and relating this to the PDMAPMA repeating units (–CH2–, either at 2.9 ppm or 3.1 ppm (c and d)).

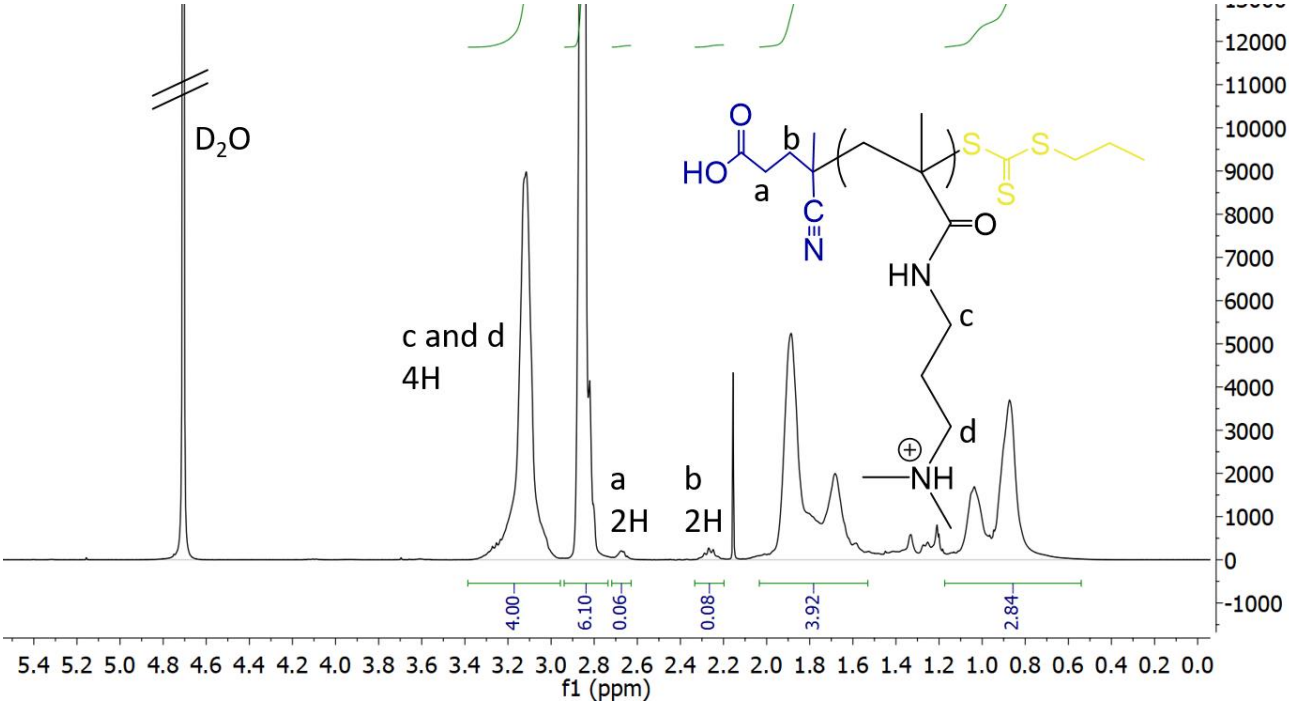


**Figure S1**. $^{1}$H-NMR spectrum of macroRAFT agent PDMAPMA dissolved in $D_2O$ and assignment of the different proton resonances. There are some peaks originating from solvent after precipitation (2.15 is acetone).

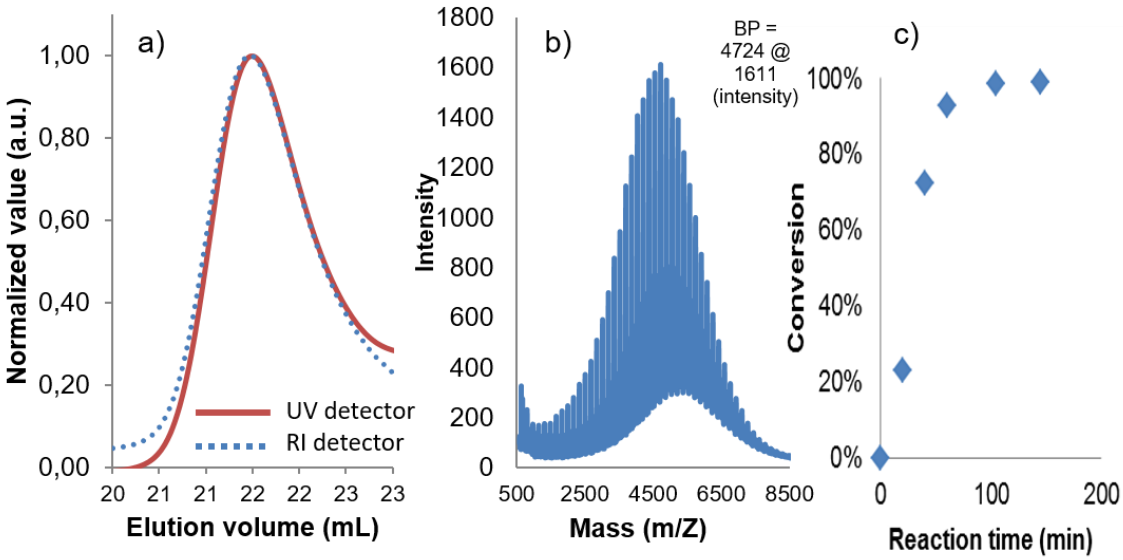


**Figure S2.** a) Chromatograms from SEC using DMSO as solvent, with normalized signals b) MALDI-ToF MS spectrum of PDMAPMA macroRAFT in water with DHB as matrix c) Conversion plot from $^{1}$H-NMR analysis (in $D_2O$) of vinyl peak disappearance relatively to 1,3,5-trioxane used as internal reference for synthesis of PDMAPMA macroRAFT in $H_2O$ with AIBA as initiator (1:5 AIBA:CTPPA ratio).

Analysis of the macroRAFT was also performed by QCM-D on silica surface to see adsorption behavior. Introducing the macroRAFT diluted to 0.1 g $L^{-1}$ in MilliQ shows adsorption, despite slight drift in baseline, resulting in a decrease in the region of 1.5 – 2 Hz, which is very low and expected due to the

high charge density (5.6 meq $g^{-1}$ from PET). Adsorption also resulted in a very low or negligible change in dissipation.

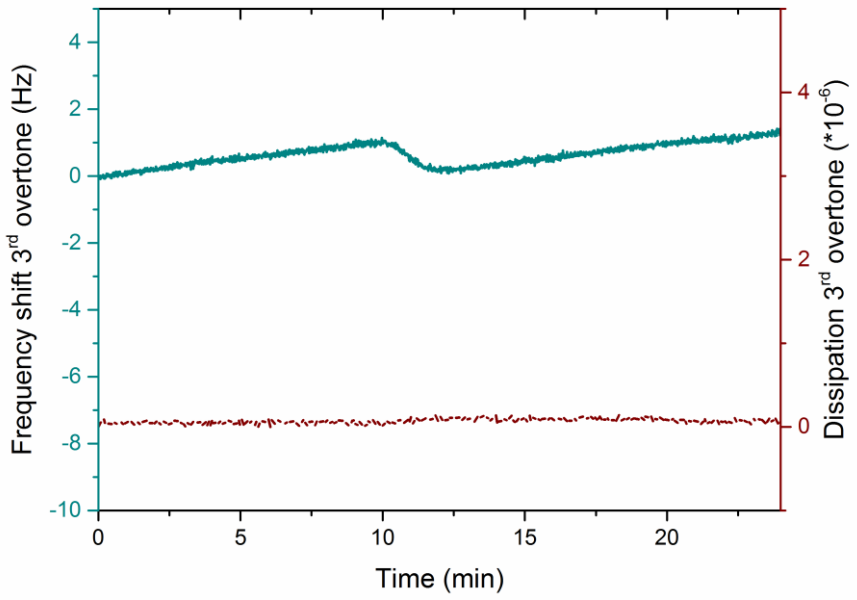


**Figure S3.** QCM-D analysis of the macroRAFT agent PDMAPMA on silica surface diluted in MilliQ water at 0.1 g $L^{-1}$. Analysis of curves for the 3rd overtone, where green line to left shows frequency change and the brown line to the right shows dissipation change. The slope of the green line is due to the small drift in the baseline during the measurement.

## 3. Analysis of PMMA, P(BA-co-MMA) and PBA latexes during synthesis and dispersions

Using macroRAFT PDMAPMA to form latexes consisting of block copolymers PDMAPMA-*b*-PMMA, PDMAPMA-*b*-P(BA-*co*-MMA) and PDMAPMA-*b*-PBA. To compare the synthesis of the different latexes, all experimental set-ups are shown below in Table S1 including concentrations of macroRAFT, AIBA initiator and monomer. Figure S4 show the results from conversion measurements, kinetics and DMF SEC curves.

The synthesis of PMMA reference latexes is also shown in Table S1 first using only AIBA, MMA and water ($PMMA_{AIBA}$) and then secondly using surfactant cetyl trimethyl ammonium chloride (CTAC) from a 25wt% water solution as stabilizer ($PMMA_{CTAC}$), using the same mass ratio of stabilizer to monomer as macroRAFT for the other latexes. The resulting latex $PMMA_{AIBA}$ in THF SEC $M_n$ at 283 000, $M_w$ at 527 000 and $Đ_N$ of 1.9, in DMF SEC $M_n$ at 295 000, $M_w$ at 744 000 and $Đ_N$ of 2.5. The $PMMA_{CTAC}$ were measured only in DMF SEC resulting in $M_n$ at 917 000, $M_w$ at 2 760 000 and $Đ_N$ as high as 3.0.

**Table S1**. Summarized data for the syntheses of latexes of PMMA, PBA and the copolymer P(BA-*co*-MMA), targeting a final dry content of 15.3 to 17.3 wt%. pH of reaction was kept at 6 and the ratio [macroRAFT]:[I] was kept at 8.25 for all reactions. For emulsion polymerization using surfactant CTAC a dry content of 15.3 wt% was targeted.

| Sample (DC, wt%) | $[macroRAFT]_0$ (mM in $H_2O$) | $[M]_0$ (M in $H_2O$)[a] | Added mL $H_2O$ | Added mL AIBA (aq) (at conc. 3.4 $gL^{-1}$) | $N_P$ ($10^{14}$ $mL^{-1}_{Latex}$)[b] |
|---|---|---|---|---|---|
| **$PMMA_{Tg120}$ latex (15.3%)** | 4.04 | 1.62 | 5.34 | 0.217 | 0.25 |
| **P(BA-*co*-MMA)$_{Tg3}$ latex (17.3%)** | 4.10 | 0.98(BA)+0.66(MMA) | 5.27 | 0.217 | 1.53 |
| **$PBA_{Tg-40}$ latex (15.3%)** | 3.23 | 1.29 | 6.74 | 0.217 | 6.12 |
| **Synthesis of reference latexes using only AIBA or with CTAC** | | | | | |
| **$PMMA_{AIBA}$ (15.3%)** | 0 | 1.8 | 5.4 | 0.223 | N.A. |
| **$PMMA_{CTAC}$ (15.3%)** | 56.2 | 1.62 | 7.7[c] | 0.326 | N.A. |

[a] The concentration of monomer, targeting degree of polymerization of 400. [b] The number of particles per mL latex is calculated from equation 1 and taking into account the $D_H$ from DLS measurements. [c] Amount of added water not including water from CTAC solution (25 wt%).

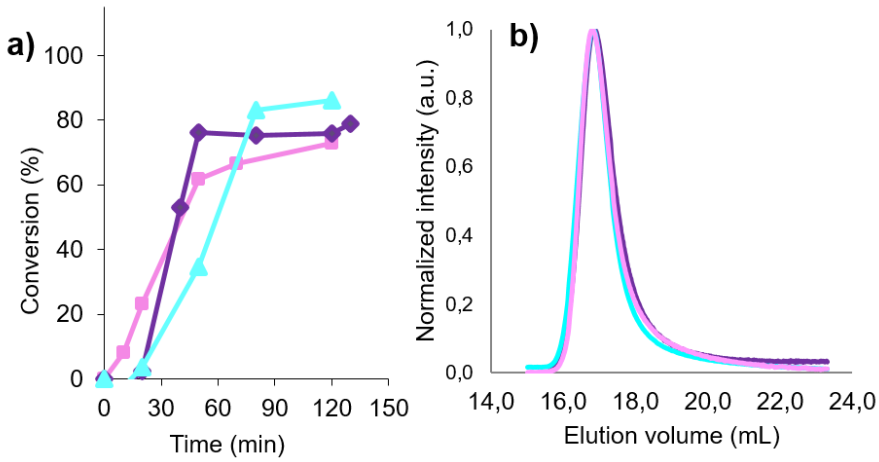


**Figure S4.** a) Monomer conversion versus time curves, and b) Chromatograms from DMF-SEC analysis of freeze-dried latexes, for PMMA latex (teal blue), P(BA-co-MMA) latex (pink) and PBA latex (purple).

All the latexes were thoroughly analyzed with DLS as can be seen below in Table S2 for the macroRAFT-mediated polymerizations, and in Table S3 for the reference latexes $PMMA_{AIBA}$ and $PMMA_{CTAC}$.

**Table S2**. DLS data from analysis of latex particles diluted into Milli-Q water and 10 mM KCl solution, before and after 3 centrifugation cycles.

| Sample | $D_H$ (nm)[a] | PdI (DLS)[a] | Zeta potential (mV)[a] | $D_H$ (nm)[b] | PdI (DLS)[b] | Zeta potential (mV)[b] |
|---|---|---|---|---|---|---|
| **$PMMA_{Tg120}$ latex** | 206 | 0.05 | 46.8 | 204 | 0.04 | 51.2 |

| | | | | | | |
|---|---|---|---|---|---|---|
| **P(BA-co-MMA)$_{Tg3}$ latex** | 156 | 0.01 | 49.1 | 163 | 0.08 | 43.9 |
| **PBA$_{Tg-40}$ latex** | 81 | 0.06 | 46.2 | 77 | 0.05 | 43.6 |
| **After 3$^{rd}$ centrifugation cycle for 60 min each time and 48 300 *g*** | | | | | | |
| **PMMA$_{Tg120}$ latex** | 218 | 0.04 | 69.1 | 199 | 0.04 | 49.2 |
| **P(BA-co-MMA)$_{Tg3}$ latex** | 164 | 0.03 | 75.4 | 152 | 0.02 | 48.5 |
| **PBA$_{Tg-40}$ latex** | 90 | 0.08 | 74.5 | 81 | 0.05 | 46.5 |

[a] Latex in MilliQ water at 0.1 g $L^{-1}$ in terms of polymer dry weight. [b] Latex in 10 mM potassium chloride at 0.1 g $L^{-1}$ in terms of polymer dry weight.

**Table S3**. DLS data from analysis of latex particles diluted into Milli-Q water and 10 mM KCl solution, before and after 3 centrifugation cycles.

| | **Before centrifugation cycle** | | | **After 3$^{rd}$ centrifugation cycle for 60 min each time and 48 300*g*** | |
|---|---|---|---|---|---|
| **Sample** | $D_H$ (nm)[a] | PdI (DLS)[a] | Zeta potential (mV)[a] | $D_H$ (nm)[b] | PdI (DLS)[b] |
| **PMMA$_{AIBA}$ (15.3%)** | 299 | 0.2 | N.A. | N.A.[c] | N.A.[c] |
| **PMMA$_{CTAC}$ (15.3%)** | 58 | 0.07 | 40.7 | 58 | 0.04 |

[a] Latex in MilliQ water at 0.1 g $L^{-1}$ in terms of polymer dry weight. [b] Latex in 10 mM Sodium chloride at 0.1 g $L^{-1}$ in terms of polymer dry weight. [c] Not possible due to the poor stability

DMF-SEC analysis of the resulting latexes before any work-up protocols using macroRAFT PDMAPMA could show a small fraction of low molar mass polymer, exemplified here for latex synthesis of P(BA-co-MMA)$_{Tg3}$, Figure S5. The low molar mass polymer seen in the chromatogram is interpreted as unsuccessful chain-extended PDMAPMA chains, a result shown before for other RAFT-mediated emulsion and dispersion polymerizations.

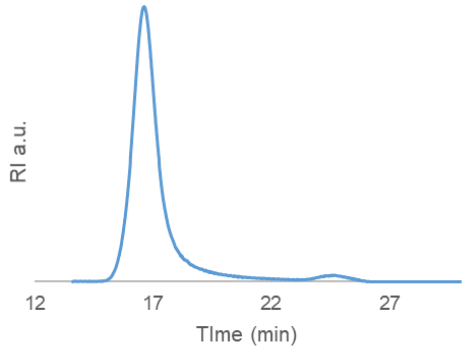


**Figure S5.** SEC results in DMF of P(BA-co-MMA)$_{Tg3}$ latex synthesized with surfactant-free emulsion polymerization using macroRAFT PDMAPMA, before any purification step. At the linger retention time region: the presence of un-extended PDMAPMA chains.

## 4. Work-up protocol for removal of free PDMAPMA-chains

The synthesis of the latexes was further evaluated by centrifugation cycles followed by a re-dispersion in deionized water to see whether residual free polymer chains were present in the water phase and if it can be removed, whilst maintaining stable latex dispersions. By successive centrifugation steps, summarized in Table S4, it was possible to decrease the amount of water soluble species from around 4-6 g $L^{-1}$ to below 1 g $L^{-1}$. Therefore, after the last centrifugation step (3$^{rd}$ centrifugation) the final latex water phase include less than the concentration calculated, see last column in Table S4.

**Table S4.** The resulting intensity from $^{1}$H-NMR in $D_2O$ of supernatant after centrifugation cycles of latexes, diluted with deionized water to half concentration as prior to centrifugation, to increase amount of material for centrifugation. Therefore, the intensity is not directly correlated with concentration in latex water phase before centrifugation and needs back-calculation from before dilution).

| Sample | Centrifugation cycle of supernatant | Intensity@ 3.1 ppm | Intensity@ 2.8 ppm | Back-calculated concentration in water phase before dilution and centrifugation [g $L^{-1}$] |
|---|---|---|---|---|
| **PMMA$_{Tg120}$ latex** | 1centr | 8960.6 | 28492.8 | 6.5 |
| | 2centr | 1764.8 | 6192.8 | 1.4 |
| | 3centr | 997.3 | 4196.2 | 0.9 |
| **P(BA-*co*-MMA)$_{Tg3}$ latex** | 1centr | 4827.0 | 15496.8 | 3.7 |
| | 2centr | 1711.2 | 5908.3 | 1.3 |
| | 3centr | 650.6 | 3037.0 | 0.6 |
| **PBA$_{Tg-40}$ latex** | 1centr | 4075.2 | 13516.6 | 4.3 |
| | 2centr | 2763.1 | 8971.9 | 1.8 |
| | 3centr | 1089.4 | 3709.1 | 1.0 |

The calculation of macroRAFT in the latex water phase, results in Table S4, was done by making a calibration curve using different concentrations of PDMAPMA analyzed in $D_2O$ (Figure S6). Selecting concentrations 0.1, 6.2 and 19 g $L^{-1}$ and looking at peaks of the macroRAFT at 2.8 ppm (two $-CH_3$) and 3.1 ppm (two $-CH_2$) two curves can be produced, both of which was linear fit with equation y = 1494.4x +112.79 (2.75 ppm) and y = 478x – 1.261 (3.1 ppm) and both achieving a $R^2$-value above 0.999. Using these equations for the curve it is possible to back-calculate the amount of residual macroRAFT in the water phase, assuming that all contribution in the $^1$H-NMR (using $D_2O$) at these peaks of the macroRAFT originates from free polymer not bound to any latexes in supernatant (confirmed to be actual from analysis of high concentrated $D_2O$ re-dispersed $PMMA_{Tg120}$ latex). The curves give rise to relatively similar results when back-calculated (difference gives error of 0 to 0.85 in g $L^{-1}$). The value from supernatant analysis shows clearly when water phase from latex consist of 1 g $L^{-1}$ macroRAFT or less.

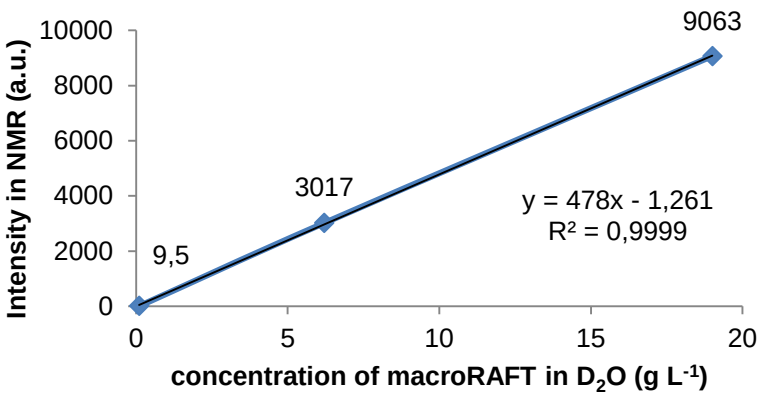


**Figure S6.** Calibration curve for macroRAFT PDMAPMA in $D_2O$ at different concentrations (0.1, 6.2 and 19 g $L^{-1}$) resulting in different intensities (here shown for the peak at 3.1 ppm). A linear fit shows the $R^2$-value for the fitted linear curve.

The residual free polymer does not only change the water phase properties such as surface tension, but also strongly affect the adsorption behavior as will be shown in the coming sections about adsorption. Using PDMAPMA macroRAFT for these systems, also gave rise to unique properties, where especially the $PMMA_{Tg120}$ latex was shown to be exceptionally easy to re-disperse into de-ionized water after pellet formation (supernatant discarded after analysis). Therefore, the impact of the corona was analyzed for $PMMA_{Tg120}$ latex comparing with the $PMMA_{CTAC}$ (cationic surfactant at wt% same as macroRAFT agent PDMAPMA for the other latexes the other sample with molar ratio was un-successful to stabilize after centrifugations (PDI in DLS above 0.2), to highlight the achieved stability of the corona, see Figure S7.

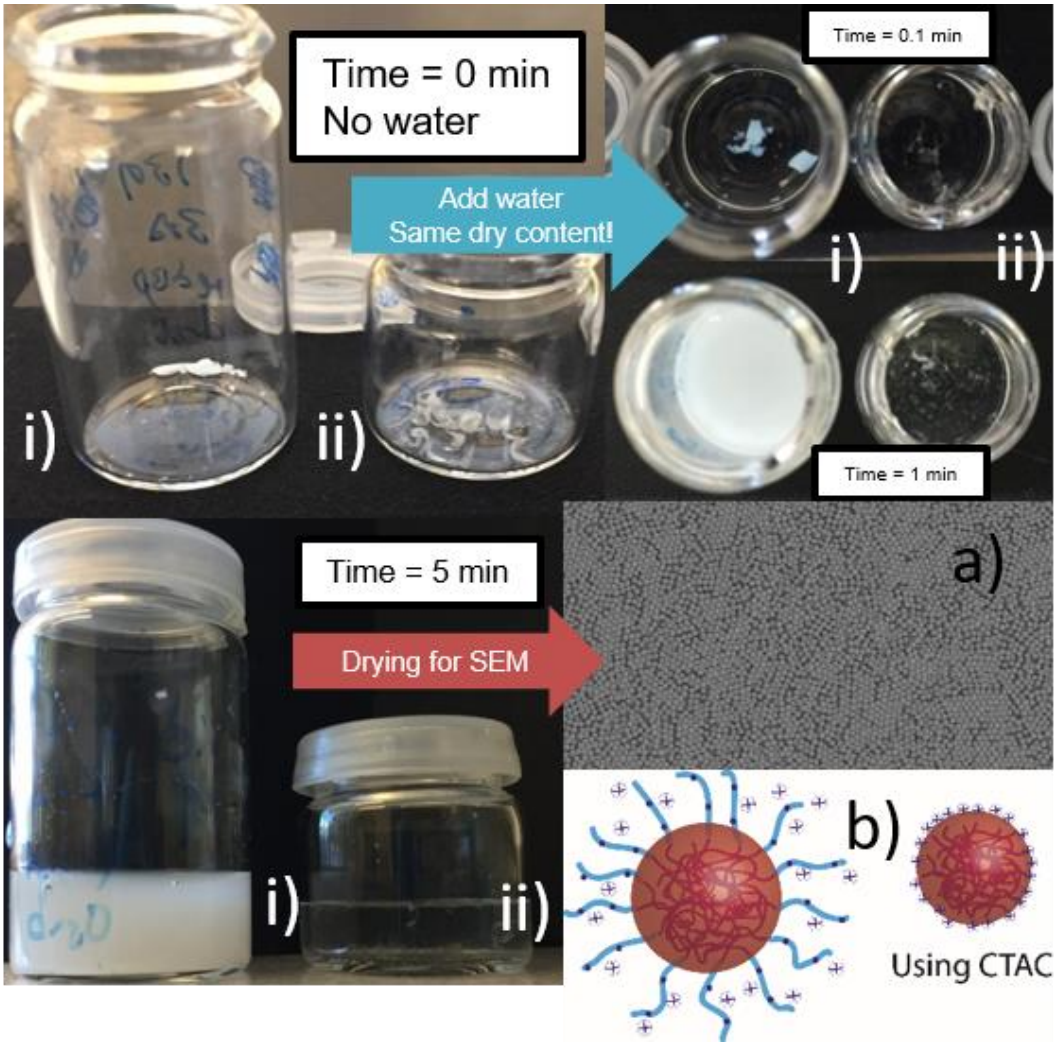


**Figure S7.** Visualizing the re-dispersion after water addition to the in ambient conditions dried latexes (without annealing). The left vial i) shows latex using macroRAFT agent PDMAPMA and the vial to the right ii) is the $PMMA_{CTAC}$ latex using commercial surfactant CTAC. The SEM image in a) shows PDMAPMA-stabilized $PMMA_{Tg120}$ latex and in b) the schematic illustration of the two latexes in water.

## 5. Adsorption in QCM-D of latexes on silica surfaces

The effect on adsorption from centrifugation protocol is summarized with the QCM-D curves below, Figure S8. The increased adsorption is very little for the two compared latexes, when using only one cycle.

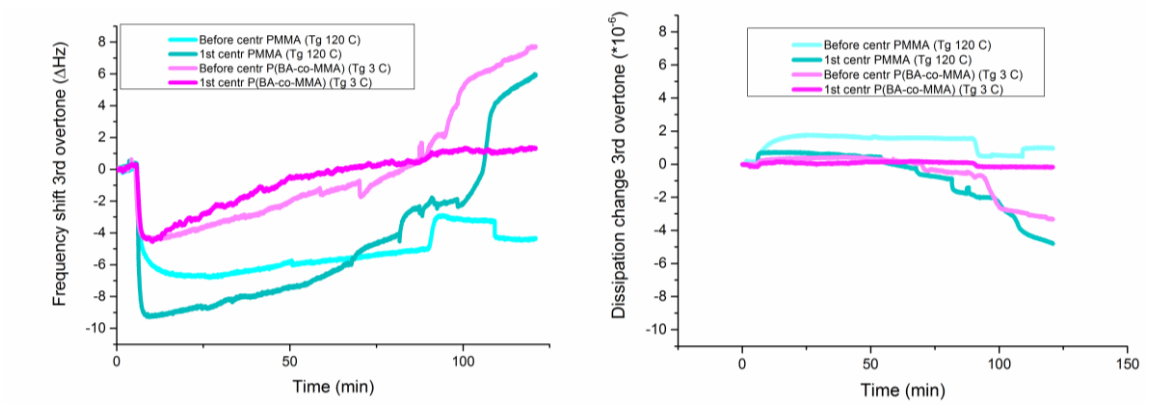


**Figure S8.** QCM-D analysis of latexes before and after 1st centrifugation cycle, adsorption on silica surface and latex in MilliQ. Rinsing step with MilliQ around 75 minutes. To the left frequency shift and to the right dissipation monitoring. The drift in baseline is seen both before and after introducing latex.

When removing the crystals from QCM-D chamber and preparing them for analysis in SEM, there is a risk that particles move during drying. Therefore, a slow drying humid atmosphere was created in a petri dish with a wet tissue for the surface analysis, as shown to prevent formation of coffee ring effect and particles aggregating due to water evaporation. See Figure S9-S10 for comparison between using different drying techniques, air gun and simple evaporation. From the SEM pictures it is clear that particles move and aggregate from the evaporation of water, caused by either a flow of air from an air gun or simply too fast drying. Despite the low mass adsorbed according to QCM-D data, there are many latexes visible on the crystal surface and this gives information about the correlation between frequency and surface coverage which might not always be the expected. A low frequency can still mean that many particles have adsorbed in number but to a low coverage percentage.

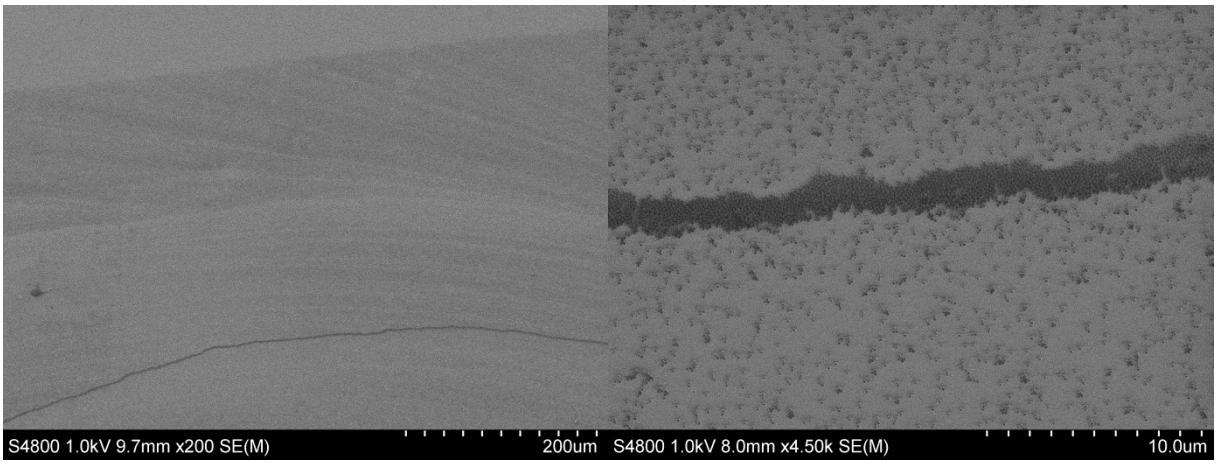


**Figure S9.** SEM images of QCM-D silica crystal surfaces after adsorption of $PMMA_{Tg120}$ latex and then dried with an air gun. To the left a zoom out to show rings and to the right zoom in on the rings that shows aggregated particles.

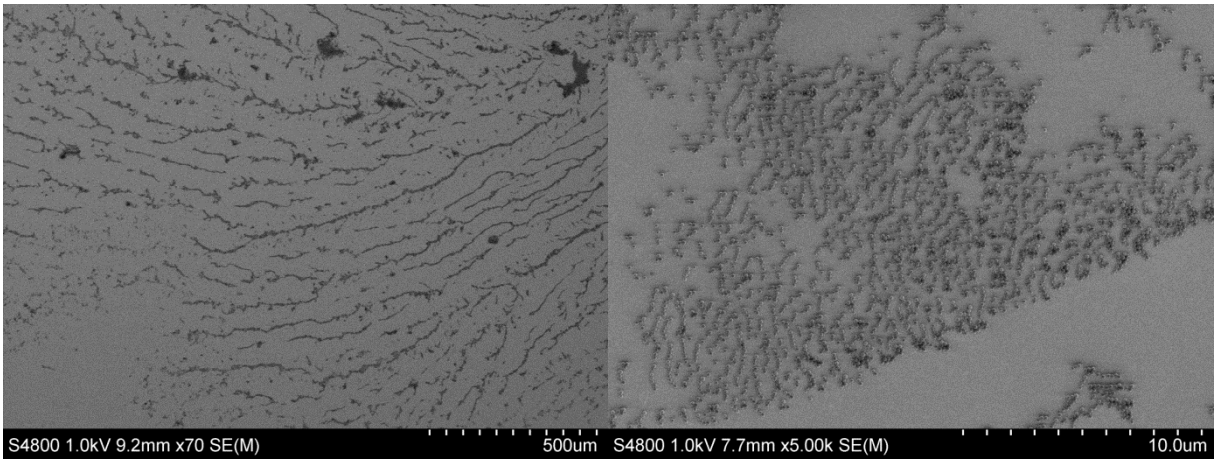


**Figure S10.** SEM images of QCM-D silica crystal surfaces after adsorption of $PMMA_{Tg120}$ latex dried in fume hood under regular air flow. Aggregation is shown as areas where a lot particles are visible in the same time as little to none particles are visible. To the left a zoom out to show "pearl necklace" formations (sample before centrifugation), to the right a centrifuged sample zoomed in.

The coffee ring effect can be decreased by using slower and careful drying as mentioned and shown to be very effective. The distribution is improved and movement of particles is decreased due to water evaporation, Figure 3 and Figure 4.

## 6. Adsorption of latexes on a CNF layer formed *in situ* with the aid of QCM-D

The latexes were characterized by CAM after the adsorption onto *in situ* formed layer of CNF on a PEI anchoring layer, Figure S11 and Table S5.

**Figure S11.** Contact angle image of the QCM-D crystal formed *in situ* with layers of PEI and CNF before subsequent treatment with $PMMA_{Tg120}$, $P(BA\text{-}co\text{-}MMA)_{Tg3}$ and $PBA_{Tg\text{-}40}$ latexes. Pictures are in the order of the mentioned latex starting from left to right, respectively.

**Table S5**. Contact angle measurement on QCM-D crystal surfaces after PEI, CNF and subsequent latex adsorption *in situ*.

| Sample | CA no annealing (°) |
|---|---|
| **No latex reference** | - [a)] |
| **$PMMA_{Tg120}$ latex** | 44 |
| **$P(BA\text{-}co\text{-}MMA)_{Tg3}$ latex** | 93 |

| | |
|---|---|
| **$PBA_{Tg-40}$ latex** | 85 |

[a)] Not performed

## 7. Adsorption of latexes on a CNF layer formed *ex situ* on silica wafers

The latexes were also characterized for their adsorption onto *ex situ* formed layer of CNF (in dispersion at 0.1 $gL^{-1}$) on a PEI anchoring layer (solution at pH 10 and at 0.1 $gL^{-1}$) mimicking the QCM-D conditions, Figure S12-S15 and Table S6. The wafers were adsorbed with latex at concentration of 0.5 $gL^{-1}$ slightly above the QCM-D concentrations for more efficient adsorption, still in 10 mM NaCl solution. The resulting surfaces were analyzed by CAM. Both before and after annealing at 160°C for 10 h to reach a thorough annealing.

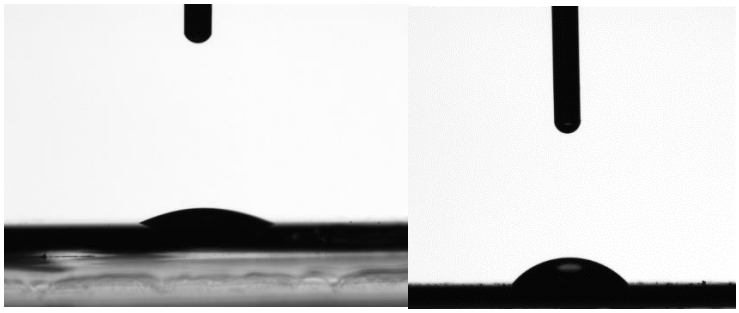

**Figure S12.** Contact angle image of the silicon dioxide wafer coated *ex situ* with layers of PEI and CNF. To the left before heat treatment and to the right after 10 h annealing at 160 °C.

**Figure S13.** Contact angle image of the silicon dioxide wafer coated *ex situ* with layers of PEI and CNF before subsequent treatment with $PMMA_{Tg120}$ latex. To the left before heat treatment and to the right after 10 h annealing at 160 °C

**Figure S14.** Contact angle image of the silicon dioxide wafer coated *e- situ* with layers of PEI and CNF before subsequent treatment with P(BA-*co*-MMA)$_{Tg3}$ latex. To the left before heat treatment and to the right after 10 h Annealing at 160 °C

**Figure S15.** Contact angle image of the silicon dioxide wafer coated *ex situ* with layers of PEI and CNF before subsequent treatment with PBA$_{Tg-40}$ latex. To the left before heat treatment and to the right after 10 h annealing at 160 °C

**Table S6**. Contact angle measurement on silicon dioxide wafers after PEI, CNF and subsequent latex adsorption performed *ex situ*.

| Sample | CA no annealing (°) | CA annealing at 160°C for 10 h (°) |
|---|---|---|
| **No latex reference (PEI-CNF)** | 22 | 52 |
| **PMMA$_{Tg120}$ latex** | 39 | 62 |
| **P(BA-*co*-MMA)$_{Tg3}$ latex** | 93 | 89 |
| **PBA$_{Tg-40}$ latex** | 85 | 93 |

# 8. Adsorption of latexes to clean glass substrates

The latexes were also adsorbed at 0.1 g L$^{-1}$ concentration onto cleaned microscopy glass slides followed by rinsing with MilliQ and analysis of the coated glass in CAM, see Figure S16 and Table S7. Figure S16 also shows the reference surface i.e. only the glass substrate. There was no heat treatment of any of the samples.

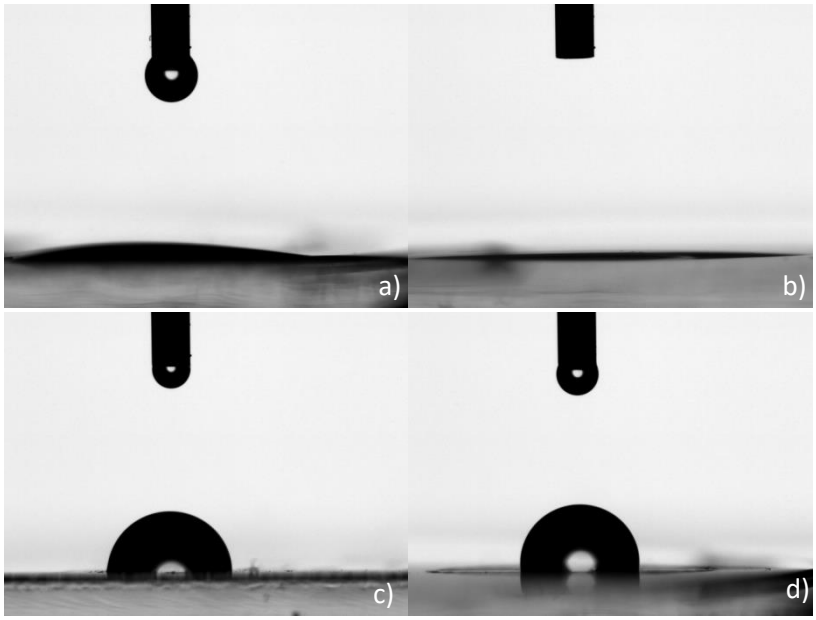


**Figure S16.** Contact angle image of the glass substrate a) without any latex coating, b) PMMATg120 latex, c) P(BA-co-MMA)Tg3 latex and d) the PBATg-40 latex.

**Table S7**. Contact angle measurement on glass substrates after latex adsorption.

| Sample | CA no annealing (°) |
|---|---|
| **No latex reference** | - [a)] |
| **$PMMA_{Tg120}$ latex** | - [a)] |
| **$P(BA\text{-}co\text{-}MMA)_{Tg3}$ latex** | 92 |
| **$PBA_{Tg\text{-}40}$ latex** | 99 |

[a)] Full wetting of the water droplet

# 9. Adsorption of latexes on filter paper

The latexes were also adsorbed at 0.1 g $L^{-1}$ concentration onto cellulose filter papers followed by rinsing with MilliQ and analysis of the filter papers with CAM (Table S8) and FTIR (Figure S17). The reference PMMA latex made with CTAC surfactant instead of macroRAFT, was also included and analyzed on filter paper, showing a hydrophobic surface already after the first milder heat treatment.

**Table S8**. Contact angle measurement on filter papers after latex adsorption.

| Sample | CA no annealing (°) | CA after annealing 140 °C 3h | CA after annealing 160 °C, over night |
|---|---|---|---|
| **No latex reference** | - [a)] | - [a)] | - [a)] |
| **$PMMA_{Tg120}$ latex** | - [a)] | - [a)] | 93 |
| **$P(BA\text{-}co\text{-}MMA)_{Tg3}$ latex** | 113 | 113 | 113 |
| **$PBA_{Tg\text{-}40}$ latex** | 137 | 137 | 137 |
| **$PMMA_{CTAC}$ reference** | - [a)] | 124 | 124 |

[a)] Full absorption of the water droplet

In Figure S17 FTIR data show clear adsorption of latexes, and an increase with added salt to the dispersions, same as shown for QCM-D data. Despite the low degree of charge compared to CNF the filter paper shows larger adsorption of latex in 10 mM NaCl.

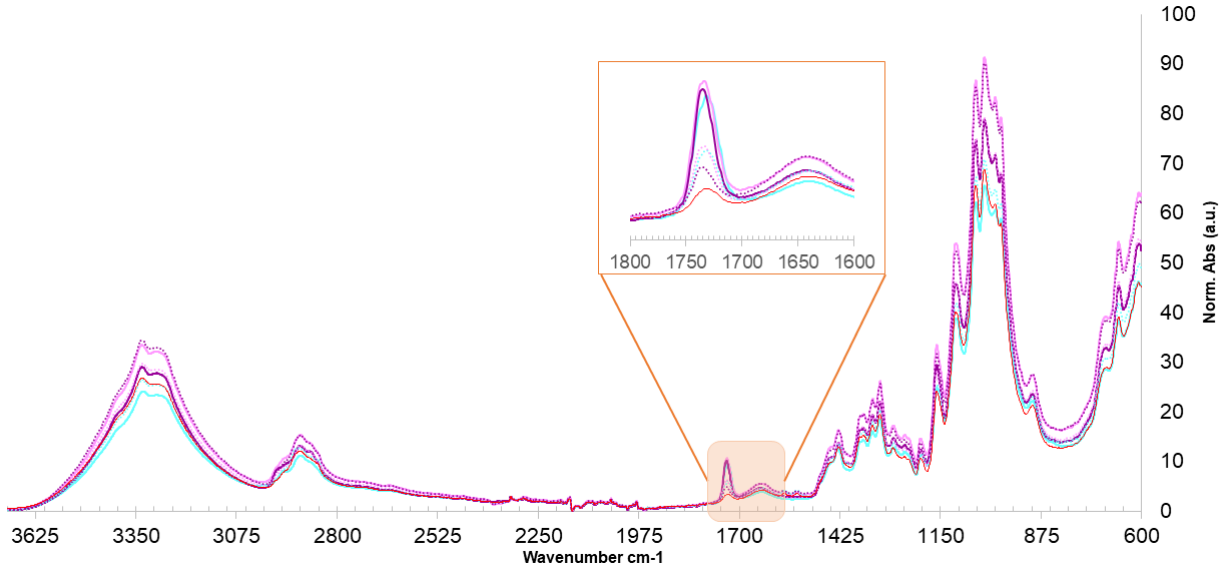


**Figure S17.** FTIR spectra of the filter papers with adsorbed latexes at 0.1 g $L^{-1}$ for 24 h, followed by a rinsing step in MilliQ for another 24 h. PMMA (teal blue), P(BA-*co*-MMA) (pink) and PBA (purple), were introduced in MilliQ (dashed lines) or 10 mM NaCl (solid lines). Red solid line shows the reference latex $PMMA_{CTAC}$ in 10 mM NaCl.